On the Onset and Control of Chaos in Hysteretic Systems Using the Bouc–Wen Model

Abel Viji George[1]
Department of Aerospace Engineering
Indian Institute Of Technology - Madras
Chennai, India
ae21b001@smail.iitm.ac.in

***Abstract*—This study investigates the onset of chaos in a nonlinear hysteretic system incorporating negative stiffness and modeled using the Bouc–Wen formulation. Building upon the analytical framework provided in previous literature, the focus is on replicating and extending the key findings related to the onset of chaotic behaviour. Using numerical integration techniques and diagnostic tools such as Poincaré sections, Lyapunov exponent analysis and 3D phase trajectory visualization, the dependence of chaos on system parameters, particularly the forcing amplitude, F_0 is examined. The results reveal critical thresholds for the appearance of horseshoe chaos and demonstrate the potential for controlling chaotic behaviour through parameter tuning. These findings offer valuable insights into the design and control of systems with hysteretic damping, with applications in structural mechanics and vibrational analysis.**

***Index Terms*—Hysteresis, Bouc-Wen Model, Negative Stiffness, Separatrix, Chaos**

I. Introduction

The study of chaotic behaviour in nonlinear dynamical systems has long fascinated researchers due to its implications for unpredictability and system stability. Among its various forms, horseshoe chaos—marked by transverse intersections of stable and unstable manifolds—represents a fundamental route to complex behaviour [1]. This study examines the onset of such chaos in a single-degree-of-freedom (SDOF) system with hysteretic restoring force, modeled using the Bouc–Wen formulation. The concept of employing negative stiffness springs, or 'anti-springs', for enhanced energy dissipation has been explored in [2].

Motivated by the work of [1], which used Melnikov analysis to predict thresholds for chaotic transitions, this study aims to replicate and extend those findings with a specific focus on the onset of chaos. Numerical simulations are conducted using MATLAB, employing diagnostic tools such as Poincaré sections, Lyapunov exponents and 3D phase trajectories to analyze the system's behaviour.

The goal is to map parameter regimes associated with chaotic dynamics and assess how hysteresis-related parameters influence system stability. In doing so, we validate theoretical predictions and provide computational tools for chaos detection, with potential applications in structural systems employing hysteretic damping.

II. Mathematical Modeling

A single-degree-of-freedom (SDOF) system consisting of a mass m, viscous damping c, and a restoring force composed of both linear elastic and hysteretic components described by the Bouc–Wen model is considered. The equation of motion under harmonic forcing is:

$$m\ddot{x}(t) + c\dot{x}(t) + H(x, z, t) = F(t) \tag{1}$$

Here, $x(t)$ is the displacement, $\dot{x}(t)$ and $\ddot{x}(t)$ are the velocity and acceleration respectively, and $H(x, z, t)$ is the total restoring force which has both linear and hysteretic components given by:

$$H(x, z, t) = \alpha k x(t) + k(1 - \alpha)z(t) \tag{2}$$

where k is the stiffness of the system, α is the post-yield to pre-yield stiffness ratio, and $z(t)$ is the fictitious hysteretic displacement governed by [3]:

$$\dot{z} = \frac{1}{D}\left(A\dot{x} - \beta|\dot{x}||z|^{n-1}z - \gamma\dot{x}|z|^n\right) \tag{3}$$

The parameters $A > 0$, β, γ, and $n > 1$ control the shape and amplitude of the hysteresis. The hysteresis loop is thermodynamically admissible if:

$$\beta \geq \gamma \tag{4}$$

The combination of β and γ decides whether the model describes a softening or hardening hysteresis loop.

$$\beta + \gamma \geq 0 \tag{5}$$

Equation (5) is when we have strain-softening behaviour. Figure 1 depict these behaviours.

The external excitation is aassumed to be harmonic, $F(t) = F_0 sin(\Omega t)$ where F_0 and Ω are the excitation amplitude and frequency of the excitation. To facilitate energy-based analysis, the equation of motion is rewritten as:

$$\ddot{x}(t) + 2\zeta\omega\dot{x}(t) + \alpha\omega^2 x(t) + \omega^2(1 - \alpha)z(t) = F(t) \tag{6}$$

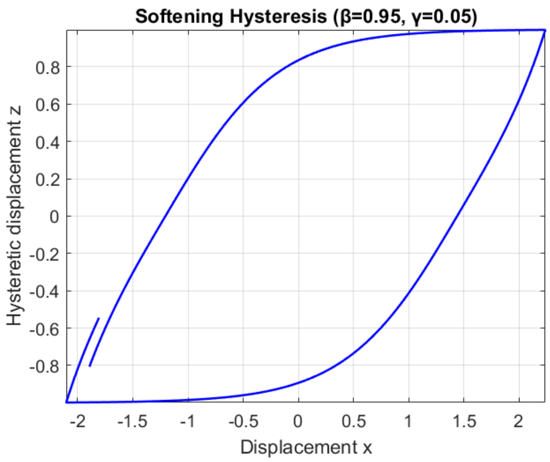

(a) Softening hysteresis loop generated by the model for $D = 1$, $n = 2$, $A = 1$, $\gamma = 0.05$ and $\beta = 0.95$

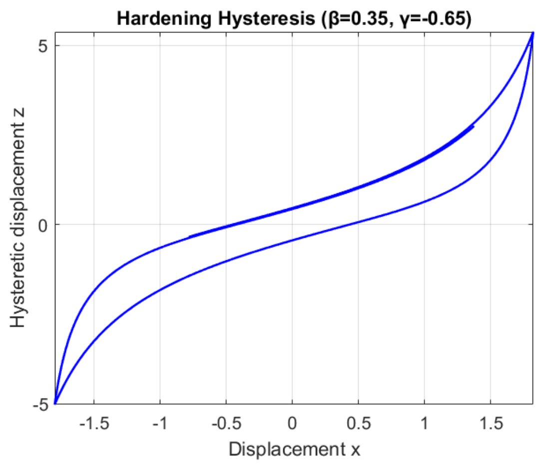

(b) Hardening hysteresis loop generated by the model for $D = 1$, $n = 2$, $A = 1$, $\gamma = -0.65$ and $\beta = 0.35$

Fig. 1: Strain-softening and hardening behaviour depending on the value of $\beta + \gamma$

with natural frequency $\omega = \sqrt{k/m}$ and damping ratio $\zeta = \frac{c}{2m\omega}$. The evolution of the hysteretic displacement z given by the following constitutive differential equation [1]:

$$\dot{z} = D^{-1} \left[A - (\gamma + \epsilon\beta) \left| z \right|^n \right] \dot{x} \tag{7}$$

where $\varepsilon = \operatorname{sgn}(\dot{x}) \operatorname{sgn}(z) = \pm 1$.

This model captures the complex nonlinear hysteretic behaviour of the system, enabling the analytical and numerical investigation of chaotic dynamics under periodic forcing.

III. Appearance of Separatrix

The system dynamics from equations (6) and (7) can be recast in state-space form for an unperturbed system with no external forcing:

$$\begin{aligned} \dot{x} &= y \\ \dot{y} &= -2\zeta y - \alpha\omega^2 x - (1 - \alpha)\omega^2 z \\ \dot{z} &= D^{-1} \left[A - (\gamma + \varepsilon\beta) |z|^n \right] y \end{aligned} \tag{8}$$

For $D = 1$ and $n = 2$, we get three fixed points as seen from Figure 2.

The potential energy of the system is given by:

$$V(x) = \frac{1}{2}\alpha\omega^2 x^2 + \omega^2 (1 - \alpha) \int z(x)\, dx \tag{9}$$

For small shape parameters, a quartic approximation of the potential is used:

$$V_{\text{ap}}(x) = \frac{1}{2} K_1 x^2 - \frac{1}{12} K_3 x^4 \tag{10}$$

where K_1 and K_3 depend on α, A, γ, β, and ω [1]. This potential leads to a monostable structure with heteroclinic orbits and this has been shown in Figure 2. The appearance of the separatrix which suggests the intersection of the perturbed and unperturbed heteroclinic orbits. This intersection suggests the onset of horseshoe chaos. So, the shape parameters of the hysteresis force have a direct link with the appearance of horseshoe chaos in the system.

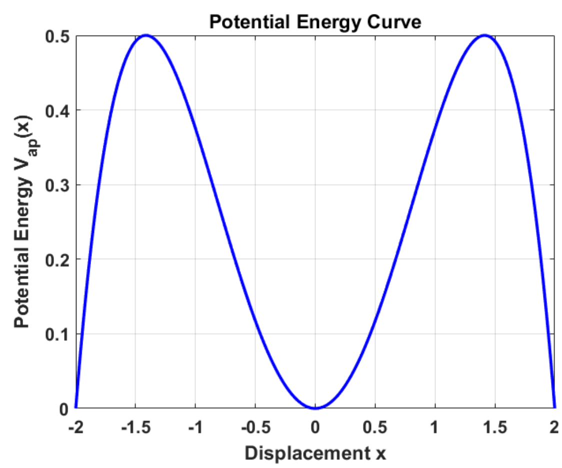

(a) Potential Energy for the unperturbed system

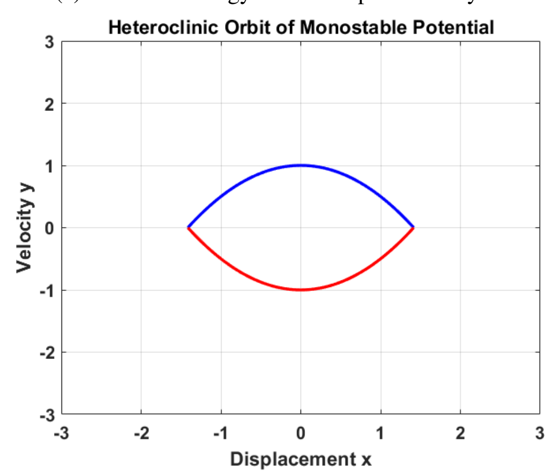

(b) Heteroclinic orbit for the unperturbed system

Fig. 2: Potential Energy Curve and heteroclinic orbit for the unperturbed case

IV. Melnikov Analysis

Melnikov Analysis is an effective method to analytically compute the threshold for the onset of horseshoe chaos in the Bouc-Wen model. For the detailed discussion, refer [1]. The Melnikov function [4] is:

$$M(\tau_0) = \int_{-\infty}^{\infty} y_{\text{het}}(\tau) \left[-2\zeta\omega y_{\text{het}}(\tau) + F_0 \cos(\Omega\tau + \tau_0)\right] d\tau \tag{11}$$

where, (x_{het}, y_{het}) are the pair of saddle points which form the heteroclinic orbit. Horseshoe Chaos occurs when $M(\tau_0)$ has simple zeros [1]. This yields a threshold condition for the forcing amplitude:

$$F_0 \geq F_{\text{CR}}(\Omega, \alpha, A, \beta, \gamma) \tag{12}$$

where the critical forcing amplitude, F_{CR} is given by,

$$F_{\text{CR}} = \left| \frac{4\zeta\omega^3 \left(\alpha + (1-\alpha)A\right)^2}{(\gamma + \varepsilon\beta)(1-\alpha)A^2\, \Omega\pi \sin(\Omega\tau_0)} \right. \\ \left. \times \sinh\left(\frac{\Omega\pi}{2\omega\sqrt{\frac{\alpha+(1-\alpha)A}{2}}}\right) \right| \tag{13}$$

Since, we have an analytical relation for F_{CR}, we can see its dependence on the parameters of the Bouc-Wen model as shown in Figure.

V. Basin of Attraction Investigation

A fundamental characteristic of the Melnikov theory is the fractality of the basin of attraction when chaos is present. In [1] the focus is on the amplitude of the external forcing as our parameter to study the onset of chaos. There are always two sets of parameters considered:

- Uncontrolled: $\epsilon = 1$, $\alpha = -0.5$, $\beta = 0.95$, $\gamma = 0.05$, $\zeta = 0.02$ and $A = 1$.
- Controlled: $A = 0.7$, $\alpha = -0.4$ and $\gamma + \epsilon\beta = 0.9$ with the other parameters same as the uncontrolled case.

The main motivation is to demonstrate that by adjusting the parameters of the Bouc–Wen model, the onset of chaos can be controlled. The Basin of Attraction (BoA) here refers to the set of initial conditions for which the system's final state remains within a predefined spatial bound. To visualize the sensitive dependence on initial conditions and identify chaotic regions, the BoA was computed via a grid-based simulation. The phase space was sampled over a fine 200×200 grid of initial positions and velocities, with each trajectory numerically integrated over time using MATLAB's stiff solver `ODE15s`. Trajectories were classified as bounded or unbounded based on final displacement and convergence rate. A color-coded map was generated by assigning values based on stabilization time or escape behavior and normalized over a continuous color scale. The resulting plot in Figure 4 reveals fractal-like boundaries between stable and unstable regions, indicating the presence of horseshoe chaos. The forcing amplitude used was

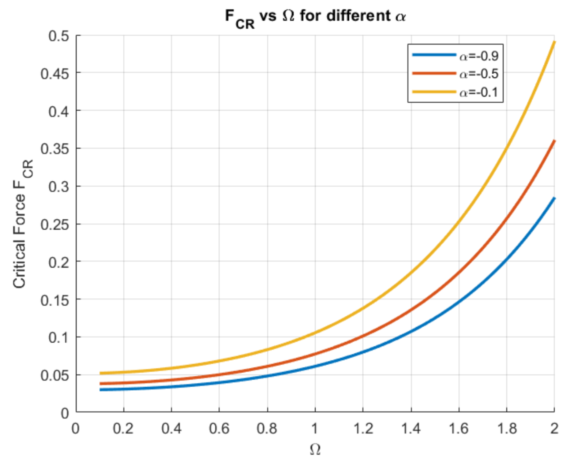

(a) F_{CR} vs Ω for different α

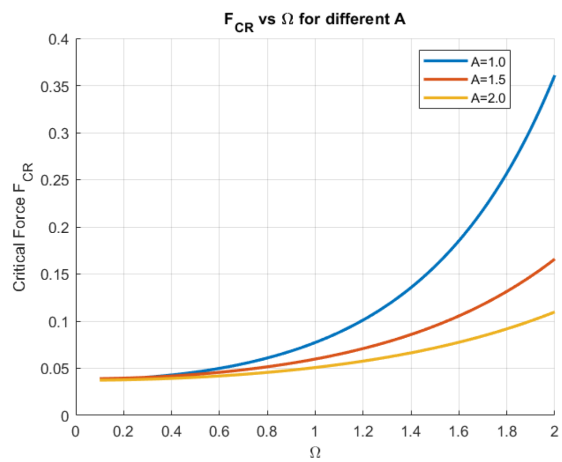

(b) F_{CR} vs Ω for different A

Fig. 3: Dependency of F_{CR} on some parameters of the Bouc-Wen model

compared against the analytical threshold F_{CR} computed via Melnikov theory to validate the regime of chaotic dynamics.

Figure 4 illustrates how varying the forcing amplitude affects the system. The Melnikov analysis (13) gives $F_{\text{CR}} = 0.0773$ for the uncontrolled parameter set. For $F_0 = 0.03 < F_{\text{CR}}$, the BoA retains a well-defined geometry, indicating non-chaotic behavior. When $F_0 = 0.25 > F_{\text{CR}}$, the BoA exhibits a fractal structure, confirming the onset of chaos. Applying a controlled parameter set for the same $F_0 = 0.25$ shows that the chaotic behavior can be suppressed, thereby confirming the effectiveness of parameter-based control in the Bouc–Wen model.

VI. Visualize Chaos in Conventional Terms

The only method explored in [1] for identifying chaos was through the fractal structure of the Basin of Attraction. As an extension, this study quantifies chaos using commonly accepted metrics such as 3D phase trajectories and Lyapunov exponents.

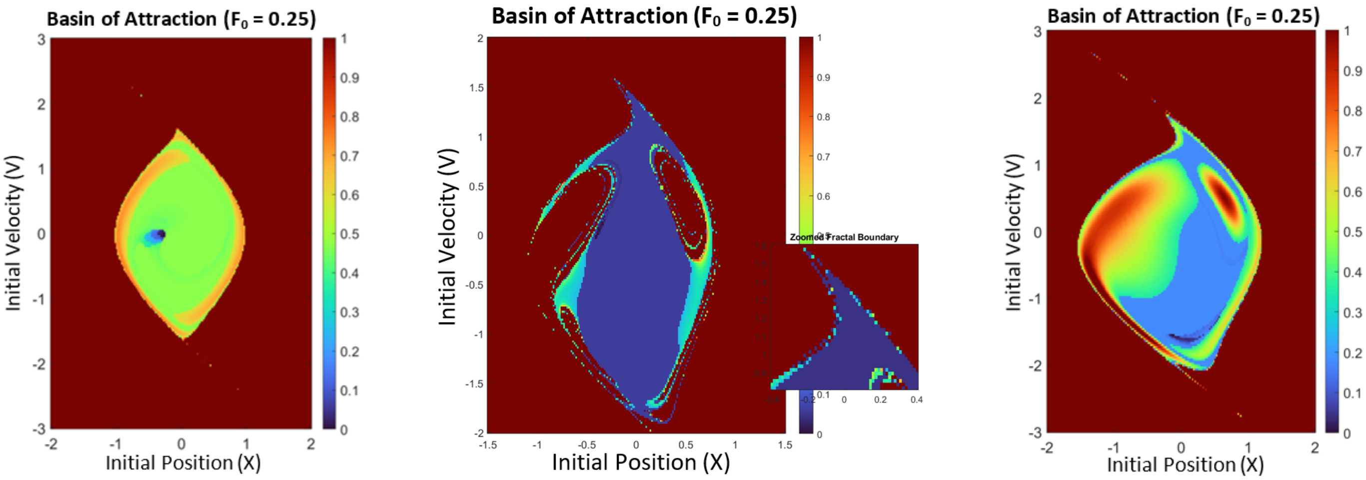

(a) Uncontrolled case, $F_0 < F_{CR}$ (b) Uncontrolled case, $F_0 > F_{CR}$ (c) Controlled case, $F_0 > F_{CR}$

Fig. 4: Showing how the onset of chaos can be controlled by varying the parameters of the Bouc-Wen model.

The first task is to examine the $3D$ phase-space trajectories spanned by x, $\dot{x}$, and z. Inspired by classical examples like the Lorenz attractor, it can be checked whether this system exhibits similarly complex behavior. Figure 5 compares trajectories for the uncontrolled cases with $F_0 < F_{\mathrm{CR}}$ and $F_0 > F_{\mathrm{CR}}$. A clear difference in dimensionality is observed, although it is inconclusive whether the system forms a strange attractor. Notably, the controlled case with $F_0 > F_{\mathrm{CR}}$ (not shown here) visually resembles the stable $F_0 < F_{\mathrm{CR}}$ case, suggesting suppression of chaotic dynamics.

Next, a Poincaré section is used to study the system's response over periodic intervals. Figure 7 shows that for $F_0 < F_{\mathrm{CR}}$, trajectories converge to a single point—indicating a limit cycle. For $F_0 > F_{\mathrm{CR}}$, the section reveals a scattered set of points with no apparent periodicity, suggesting chaotic behavior. However, due to lack of clarity, this alone is not conclusive. Interestingly, zoomed views of the Poincaré map reveal self-similar patterns, a feature often associated with chaos [5].

Finally, Lyapunov exponents are computed for three cases and shown in Figure 6. These plots illustrate the evolution of the separation $\delta(t)$ between initially close trajectories. The exponent is nearly zero for the non-chaotic cases (uncontrolled $F_0 < F_{\mathrm{CR}}$ and controlled $F_0 > F_{\mathrm{CR}}$), while it is positive for the uncontrolled $F_0 > F_{\mathrm{CR}}$ case—clearly indicating chaotic behaviour. This confirms that control via parameter tuning can effectively suppress chaos.

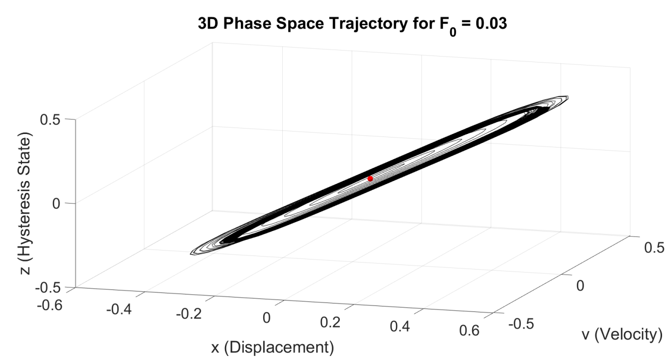

(a) $F_0 = 0.03$, uncontrolled

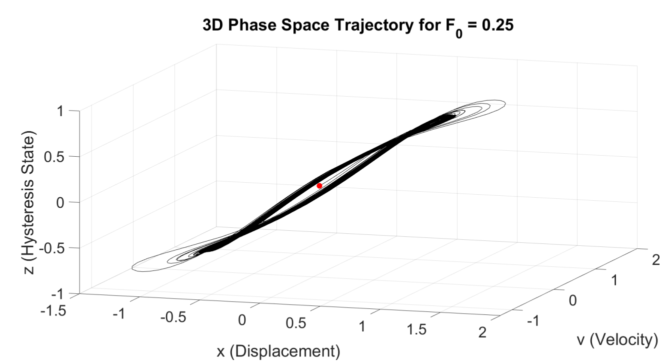

(b) $F_0 = 025$, uncontrolled

Fig. 5: Comparing the $3D$ phase trajectories for the cases with and without chaos.

VII. Conclusion

This study explored the onset and control of chaos in a nonlinear hysteretic system governed by the Bouc–Wen model with negative stiffness. Using both analytical tools such as Melnikov analysis and numerical techniques like basin of attraction mapping, phase space trajectories, and Lyapunov exponent computation, the dynamic response of the system was thoroughly investigated.

It was shown that the shape parameters of the hysteresis function have a direct influence on the appearance of horseshoe chaos. The derived analytical threshold for chaotic motion, F_{CR}, served as a useful predictor for the onset of chaotic dynamics under harmonic excitation. Through extensive MATLAB simulations, the fractal nature of the basin of attraction

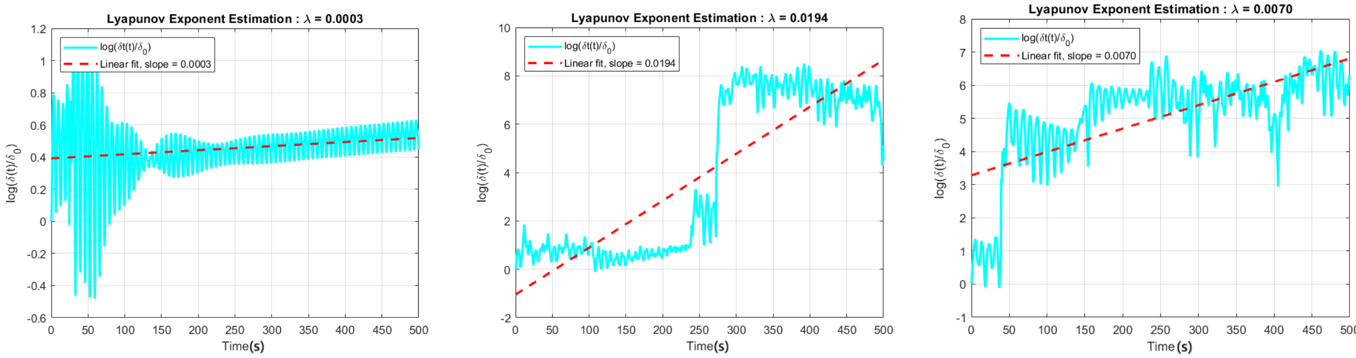

(a) Uncontrolled case, with $F_0 < F_{CR}$

(b) Uncontrolled case, with $F_0 > F_{CR}$

(c) Controlled case, with $F_0 > F_{CR}$

Fig. 6: Lyapunov Exponent plots showing how the onset of chaos can be controlled by varying the parameters of the Bouc-Wen model.

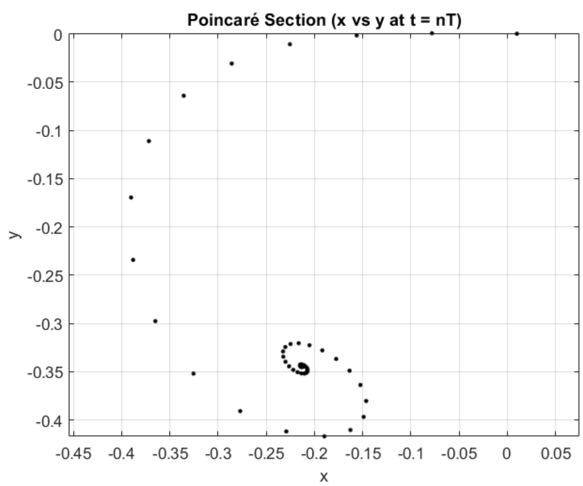

(a) $F_0 < F_{CR}$, uncontrolled case

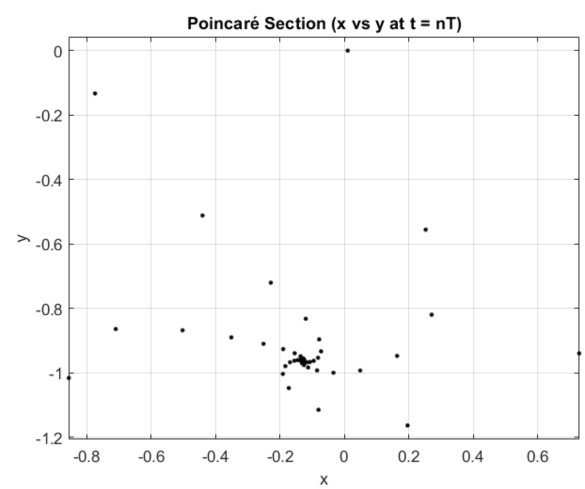

(b) $F_0 < F_{CR}$, uncontrolled case

Fig. 7: Poincaré sections for the uncontrolled case

was clearly observed when the forcing amplitude exceeded this critical value.

Additionally, the system's behaviour was visualized using conventional chaos diagnostics. The 3D phase trajectories and Lyapunov exponent analysis confirmed that chaos could be mitigated or entirely suppressed by tuning the hysteretic parameters — effectively demonstrating a mechanism for controlling nonlinear instability.

These findings reinforce the importance of hysteretic parameter design in structural and mechanical systems where chaos may pose safety or performance concerns. Future work may involve exploring in depth the self-similar nature of the Poincaré sections and understanding if there are specific patterns formed in the phase trajectories similar to the Lorenz strange attractors. Another route to pursue would be to check if chaos can be controlled by varying other parameters of the model apart from the forcing amplitude as was done in this study.

REFERENCES

[1] O. N. Y. Ngouoko, B. R. Nana Nbendjo, and U. Dorka, "On the appearance of horseshoe chaos in a nonlinear hysteretic systems with negative stiffness," *Archive of Applied Mechanics*, vol. 91, no. 11, pp. 4621–4630, 2021.

[2] C. Geo and E. Charalampakis, "A new hysteretic nonlinear energy sink (hnes)," *Communications in Nonlinear Science and Numerical Simulation*, vol. 60, pp. 1–11, 2018.

[3] F. Ikhouane and J. Rodellar, "On the hysteretic bouc-wen model. part i: Forced limit cycle characterization," *Nonlinear Dynamics*, vol. 42, pp. 63–78, 2005.

[4] S. Wiggins, *Introduction to Applied Nonlinear Dynamical Systems and Chaos*. New York: Springer, 1990.

[5] A. Shahhosseini, M.-H. Tien, and K. D'Souza, "Poincaré maps: a modern systematic approach toward obtaining effective sections," *Nonlinear Dynamics*, vol. 111, pp. 529–548, 2023.